UNIVERSITY OF CALIFORNIA SAN DIEGO

An Evaluation of a MYOTON Device as a Means for Spaceflight Monitoring of Muscular Biomarkers

A thesis submitted in partial satisfaction of the requirements for the degree Master of Science

in

Biology

by

Joseph Siprut

Committee in charge:

Professor Lonnie Petersen, Chair
Professor Shelley Halpain, Co-Chair
Professor Elina Zuniga

2021

The thesis of Joseph Siprut is approved, and it is acceptable in quality and form for publication on microfilm and electronically.

University of California San Diego

2021

DEDICATION

I would like to dedicate this thesis to my brother, Arthur Siprut. His uniqueness and artistic creativity bring so much light into my life. I am incredibly grateful to have him as a brother.

EPIGRAPH

"Do not go gentile into that good night.

Rage, rage against the dying of the light."

- Dylan Thomas

TABLE OF CONTENTS

LIST OF ABBREVIATIONS

MT = Muscle Tone

MS = Muscle Stiffness

ME = Muscle Elasticity

PSM = Paraspinal Muscles

ACKNOWLEDGEMENTS

I would like to thank Dr. Petersen for her unwavering support, guidance, and patience throughout this difficult year. She has been the best mentor I could have ever asked for, and I would not be the person I am today without her. I am forever grateful for the opportunities she has provided me with. I would also like to thank her for assisting me in creating this project and for serving as principal investigator.

I would also like to acknowledge and thank Justin Lee and Elizabeth Heyde for their help in data collection, study design, and guidance. Aside from their wonderful senses of humor and intellectual contributions, they are amazing people to work with. I am incredibly grateful for you both.

I'd like to thank Adidtya Vasan and Dr. James Friend for graciously allowing us to use their equipment and lab space.

Lastly, I would like to thank any and all family and friends who have supported me throughout this process. This pandemic year has been incredibly difficult, and I would not have been able to get through it without their love and support.

ABSTRACT OF THE THESIS

An Evaluation of a MYOTON Device as a Means for Spaceflight Monitoring of Muscular Biomarkers

by

Joseph Siprut

Master of Science in Biology

University of California San Diego, 2021

Professor Lonnie Petersen, Chair
Professor Shelley Halpain, Co-Chair

Musculoskeletal deconditioning is a significant risk during long-term spaceflight. In this study, we evaluated the use of a MYOTON probe for spaceflight monitoring of muscular biomarkers. The probe provides data on muscle tone (MT) in Hz, Muscle Stiffness (MS) in N/m, and Muscle Elasticity (ME) via logarithmic decrement. Our initial question was whether use of a guiding belt for the MYOTON probe to measure the paraspinal muscles (PSM) can improve data reliability and accuracy during repeated measurement. The belt significantly reduced standard deviations for ME. Additionally, by comparing our belt data to data on lateral and vertical biomarker deviation, we were able to conclude that use of the guiding belt improves data reliability by measuring at a more appropriate area of the spine. As a second

experiment, we wanted to evaluate the extent to which subcutaneous fat thickness can confound MYOTON muscular biomarker data. By applying a quadratic regression model to our data on subcutaneous fat thicknesses at various anatomical loci, we were able to conclude that .689 ± .035 cm is the maximum fat thickness before MYOTON data become confounded and are no longer valid. Our final experiment aimed to determine if resistance exercise can confound MYOTON data. We found immediate increases in MT and ME following completion of the exercise protocol. All biomarker values returned to baseline within 10 minutes post exercise completion. These experiments help further human spaceflight progress by validating the use of a MYOTON probe for safe and effective monitoring of muscular biomarkers.

1 INTRODUCTION

Muscular deconditioning due to weightlessness is a major physiological risk of long-term spaceflight (Fitts et al, 2000). The effects of this spaceflight associated muscular atrophy are most pronounced when astronauts return to earth, and in some cases can significantly affect quality of life (Mulavara et al, 2018). These musculoskeletal alterations can also potentially impact performance on mission critical tasks such as extra vehicular activity and emergency situations. Extended periods of time spent in weightlessness has also been shown to impact whole body motor control upon returning to the gravitational field on Earth (Mulavara et al, 2010).

Under normal physiological conditions, human resting muscle tone (MT) has significant postural and stabilizing implications while only making up approximately 1% of maximal voluntary contraction. Because humans have evolved under the gravitational forces on Earth, the human body has adapted to maintain a systemic degree of resting MT to counteract the constant force of gravity. Under weightlessness however, the musculoskeletal system loses the need to maintain resting MT due to the absence of a constant gravitational stress (Tanaka et al, 2017). Because muscles require regular use for their development and maintenance, loss in MT associated with weightlessness can cause significant muscular atrophy. Post-spaceflight studies have found quadriceps muscle volume decreases up to 6.0%, anterior calf by 3.9%, soleus-gastrocnemius by 6.3%, hamstrings by 8.3%, and paraspinal erectors by 10.3%. Additionally, these decreases in muscle volume remained significantly below baseline at 2 weeks post recovery (LeBlanc et al, 1995; Akima et al, 2000).

Human skeletal muscle can be classified as slow fiber type 1 or fast fiber type 2a, 2b and 2x. These classifications are based on myosin heavy chain isoform pattern and relative oxidative capacity (Fitts et al, 1995). Because slow twitch type 1 fibers have a high oxidative capacity, they can be active for long durations of time. This makes them ideal for constantly active postural muscles and muscles used for low intensity exercise such as walking or jogging. In contrast, type 2 fibers have low oxidative capacity and

high glycolytic capacity, making them well suited for intense locomotive activity such as weightlifting or sprinting (Armstrong et al, 1982; Suzuki et al, 1988; Smith et al, 1977; Gilman et al, 1983). Postural type 1 slow twitch muscles such as the paraspinal muscles (PSM) experience full unloading under weightlessness, and for this reason they are most susceptible to atrophy caused by spaceflight (Fitts et al, 2000).

Several studies have been conducted examining mechanisms of muscle atrophy associated with spaceflight. Data has shown that within the first week of spaceflight, slow twitch type 1 fibers decrease while the number of fast twitch fibers increase (Edgerton et al, 2008). This observation aligns itself with our understanding of fiber type functionality since type 1 postural fibers are unloaded in weightlessness and type 2 fiber usage increases due to the locomotive demands required in space. To further study this observation, Haddad et al aimed to quantify changes in myosin heavy chain isoforms after 9 days of weightlessness in rats. They found that the relative concentration of type 1 and 2a myosin heavy chains decreased significantly and were offset by increases in type 2b and 2x myosin heavy chains (Haddad et al, 1993).

Reductions in muscle mass have also been shown to be accompanied by reductions in total sarcoplasmic protein and mRNA content (Steffen et al, 1986). Ferrando et al further studied this question by conducting a 14-day study under simulated weightlessness (-6 degrees head down tilt bed rest). They found whole body lean mass was reduced but not accompanied by reductions in serum cortisol, insulin, insulin-like growth factors, and testosterone. Instead, they found that reduced total protein synthesis was the primary driver in muscle volume loss (Ferrando et al, 1996). These results have been supported by several other studies (Leblanc et al, 1992; Stein et al, 1999; Stein and Leskiw et al, 1999; Stein and Schluter et al, 1999; Baldwin et al, 1996). Furthermore, a study done by Allen et al observing muscular gene expression in a murine model quantified changes in mRNA levels under weightlessness using real-time polymerase chain reaction and compared them to controls under normal gravity. They found significant reductions in growth factor mRNA levels of PIP-3 kinase, insulin response substrate-1,

forkhead box O1 transcription factor, PPAR-α, and PPAR-γ (Allen et al, 2008). Taken together, these studies indicate that weightlessness associated muscle atrophy is primarily regulated at the genetic level.

Neurological changes have also been observed and are thought to play a role in spaceflight associated muscular atrophy. After rats were exposed to 14-days of weightlessness, it was found that neuromuscular junctions had fewer synaptic vesicles at axon terminals, vacancy of axonal spaces, degenerative changes, and malign axonal sprouting (D'Amelio et al, 1998). While this may suggest that muscular atrophy under weightlessness may be affected by neurological alterations, research on the subject is limited and requires further study.

The molecular basis of muscle atrophy under normal gravity has also been well studied and is worth making note of. Both muscle RING finder 1 (MuRF1) and muscle atrophy F-box (MAFbx/antrogin-1) are E3 ubiquitin ligases specific to muscle whose transcriptional expression is increased under conditions inducing muscular atrophy (Bodine et al, 2014). These factors are encoded in the MAFbx gene and are activated by the glucocorticoid receptor Foxo transcription factor pathway. Decreased activity in the PI3K/AKT pathway has also been found to increase expression of antrogin-1 and can be a cause of muscular atrophy. This mechanism can be inhibited by IGF-1 treatment or AKT overexpression. Both inhibit Foxo transcription and contribute to activation mTORC1, a kinase that plays a major role in muscular anabolism, cell growth, and protein synthesis. Resistance exercise has also been found to stimulate these anabolic pathways. Thus, inhibition of Foxo and other related factors that increase antrogin-1 expression are attractive molecular targets for combating muscular atrophy (Sandri et al, 2004; Ebert et al, 2019). For these reasons, physical training has been the primary countermeasure for astronauts to combat physiological deconditioning during spaceflight (James A et al, 2015).

The risk of muscle atrophy caused by spaceflight warranted the development of technology that can monitor muscular biomarkers non-invasively. A MYOTON probe has been created for this purpose of assessing muscular quality. A non-invasive FDA approved device, it places a .58 N impulse on a muscle to produce an oscillatory motion. This provides data on muscle tone (MT) in Hz, Muscle Stiffness (MS) in N/m, and Muscle Elasticity (ME) via logarithmic decrement of the dampening oscillatory motion

(Myoton.com/technology). This device has been validated for its use under weightlessness (Schneider et al, 2014).

Because MYOTON is a novel device, the creation of a protocol for its spaceflight use and an evaluation of its limiting parameters is necessary. In this study we sought to answer questions related to its use in spaceflight through a series of related experiments.

To use the MYOTON in space, crew on the International Space Station will have to perform self-measurements. This would rely on inexperienced operators that may introduce confounding variables. Furthermore, due to their location behind the body, reliable data collection with the MYOTON probe is not possible due to anatomical constraints. The use of an operator may allow for data collection, but placing the probe in a consistent location along the PSM may be difficult. For this reason, we designed and 3D printed a MYOTON guiding belt to allow for consistent data collection of PSM biofactors. We then asked the question whether the use of a guiding belt for the MYOTON probe to measure the paraspinal muscles (PSM) can improve data reliability and accuracy. Because the PSM are one of the most affected during spaceflight, a means of monitoring them is necessary (Green et al, 2018). Additionally, per request of the French Space Agency and NASA, this belt contains and additional housing for a remotely controlled ultrasound (Arbeille et al, 2018; Garcia et al 2018; Arbeille et al, 2016). However, we did not have access to this device for this study. We therefore validated it's use through testing of a ButterflyIQ ultrasound with the belt. The belt is planned for use on the international space station in future missions. We hypothesized that, when compared to hand guided measurements, usage of this guiding belt will reduce the standard deviations of our MYOTON data and allow for measurements at more appropriate areas of the PSM.

Since MYOTON measurement of muscular biomarkers is a non-invasive procedure, it is dependent on indirect contact with muscle through the dermal layers of the skin. We therefore wished to assess the extent to which subcutaneous fat thickness can confound MYOTON data. To answer this question, we aimed to determine confounding effects that subcutaneous fat thickness can have on MYOTON detection of changes in muscular biomarkers between relaxed and contracted states. Defined as the layer of adipose

tissue underneath the dermis of the skin, fat contained in the subcutaneous region makes up 80% of all body fat. This tissue is non-myogenic and generally functions as insulation or a protective layer (Ibrahim et al, 2009). The thickness of the subcutaneous fat layer can be visualized via a line measurement function in a ButterflyIQ ultrasound visualization system. We hypothesized that as the thickness of the subcutaneous fat increases, the ability to detect statistically significant changes ($p < .05$) in muscle biomarkers between relaxed and contracted states will be diminished.

As a countermeasure to prevent physiological deconditioning, astronauts have adopted a strict exercise regimen. Prior literature has shown that exercise causes local increases in blood flow along with increased muscular stiffness and tone (Suchomel et al, 2018). This may cause a "wash-out" effect whereby local muscle tone is increased for a period of time after the completion of the exercise. Since MYOTON measurements will be performed on the international space station in the near future, we wanted to determine if post exercise increases in muscle tone due to hypertrophy can confound MYOTON muscular biomarker data. We hypothesized that, following resistance exercise, MYOTON biomarker data will be affected for several minutes before returning to baseline.

It is important to note that due to restrictions put in place by COVID-19, we were significantly restricted in our ability to recruit subjects. Thus, we were limited to only collecting data on one subject. This research should therefore be treated as laying the groundwork for future studies that will take place once COVID restrictions are lifted.

2 MATERIALS

Mytonometry involves placing a non-invasive 3mm probe perpendicular to the desired muscle. A series of impulses (precompression constant load 0.18N plus impulse 0.40 = 0.58 [N]) create a dampening oscillatory function, yielding data on muscle tone, stiffness, and elasticity. Muscle Tone (MT), measured in Hz, is the oscillation frequency of the muscle. Higher values are correlated with increased MT. Muscle Stiffness (MS), measured in newtons per meter N/m, is the resistance to a force or contraction that alters the resting state of the muscle (in this case the probe). Higher values correlate to increased MS. Muscle Elasticity (ME), measured via logarithmic decrement (the inverse of the ratio between two successive maximums in a dampening harmonic oscillating motion), is defined as the ability of the muscle to recover its original shape after an external force is applied to it. As the decrement of the muscle decreases, the elasticity increases. A decrement value of zero would equate to a perfectly elastic muscle and the harmonic oscillation would theoretically have no dampening. Lower values equate to higher elasticity values of the muscle. Myoton is FDA approved (myoton.com/technology).

ButterflyIQ ultrasound imaging utilizes high frequency sound waves (above 20 KHz) created by piezoelectric crystals in the transducer. These emitted waves enter the tissue and are reflected whenever there is a change in density or a tissue boundary. Using the speed of sound at the time the reflection hits the transducer, the distance between the ultrasound and desired tissue can be calculated. These data can then be used to generate a two-dimensional image. During an ultrasound exam, a gel is applied to the skin to prevent air pockets from forming that can block ultrasound waves. Ultrasound imaging allows for non-invasive observation of internal tissues; however, it cannot penetrate through air filled mediums such as bone and lungs (Shriki et al, 2014).

A custom 3D printed belt was used as a guide for ultrasound and Myoton measurements in order to minimize data point spread.

3 SUBJECTS

Protocol has been approved by the Institutional Review Board at UC San Diego. Due to restrictions put in place by COVID-19, a total of one subject (N = 1, 22 years, 75.75 kg, 172.7 cm) was recruited for this study. To offset this limitation, repeated trials were performed on this same subject to ensure adequate data acquisition. This subject was informed of the purpose of the study and risks associated with it. Written consent was obtained through consent forms. Requirements to participate in this study were no previous history of spinal or muscular surgery. Subjects experiencing musculoskeletal discomfort had the option of discontinuing the study. In the cases where multiple operators were used, all individuals adhered to COVID-19 precautionary guidelines set forth by the CDC.

4 STATISTICS

All statistics were performed in Prism Graph Pad. Statistical significance tests were done via a 2-tailed paired t-test. P-values less than .05 were given statistical significance.

5 EXPERIMENT 1

5.1 Study Design

Prior to participating, the subject was informed of the procedures, risks, and purpose of the study. Once consent had been provided, the subject was instructed to lay down in the prone position. Data acquisition occurred in two phases. The first phase involved MYOTON measurements of the PSM without the use of a guiding belt. To simulate the diversity of personnel in spaceflight conditions, two operators for data collection were used. By allowing for cross operator comparisons of data collected without the belt, this ensured that operator memorization of a spot along the PSM was not a confounding variable.

The second phase consisted of taking MYOTON measurements with the aid of a guiding belt. To simulate separate measurements taken during spaceflight, the belt was taken off and put back on between repeated measurements in each trial. For anatomical consistency, the subject was instructed to place the guiding belt at the narrowest region of the waist and adjust it to be as tight as possible. Each trial consisted of 10 repeated measurements both with and without the guiding belt and was performed by each of the two operators. A total of 6 trials were conducted with each operator (total trials = 12).

Data collected for MT, MS, and ME was then compiled and compared to determine if a statistically significant difference in biomarkers was observed. A p-value less than .05 was considered statistically significant. Additionally, average standard deviations of data collected with and without a guiding belt were compared to test for statistically significant differences.

As a controlled variable, we wanted to determine to what extent MYOTON biomarker data was influenced by lateral and vertical movement away from a reference point on the PSM. To do so, we collected MYOTON data at a selected location in the center of this muscle group and repeated this measurement at loci 1 cm and 3 cm laterally, rostrally, and caudally away from the location of the original measurement. These data served as a basis of comparison to determine if data collected both with and without the belt was on an appropriate area on the PSM.

In addition to comparing MYOTON biomarker data, we wanted to confirm location consistency of the guiding belt by comparing ultrasound images taken across operators both with and without a guiding belt. The subject was instructed to lay in the prone position and ultrasound gel was applied in the desired location along the spine. Ultrasound images were then captured by both operators both with and without the use of the guiding belt. They were then compared through qualitative visualization.

5.2 Results

For MT, the mean value without the use of a guiding belt was 17.26 ± 1.44 Hz. With the use of a guiding belt, the mean value for MT was 19.47 ± 1.051 Hz. This difference was statistically significant ($p < .0001$, Figure 1). Upon comparing the distribution of standard deviations, the average standard deviation without a belt was .954 ± .378 Hz, and with a belt this value decreased to .771 ± .199 Hz. However, this difference was not statistically significant ($p = .2042$, Figure 2).

For ME, the mean value without the use of a guiding belt was 1.169 ± .268. With the use of a guiding belt, the mean value for ME was .973 ± .102. This difference was statistically significant ($p < .0001$, Figure 3). Upon comparing the distribution of standard deviations, the average standard deviation without a belt was .152 ± .047, and with a belt this value decreased to .074 ± .022. This difference was statistically significant ($p = .001$, Figure 4).

For MS, the mean value without the use of a guiding belt was 342.5 ± 57.1 N/m. With the use of a guiding belt, the mean value for MS was 413.9 ± 40.78 N/m. This difference was statistically significant ($p < .0001$, Figure 5). Upon comparing the distribution of standard deviations, the average standard deviation without a belt was 35.32 ± 16.49 N/m, and with a belt this value decreased to 30.18 ± 6.914 N/m. However, this difference was not statistically significant ($p = .361$, Figure 6).

We measured the deviation in MT at points laterally, rostrally, and caudally away from a reference point on the PSM. The data collected at these differing points were then compared to the reference point for statistical significance ($p < .05$, Figure 8). At the reference point, mean MT was 18.34 ± 1.385 Hz. At

a point 1cm laterally, MT was 15.18 ± .08 Hz ($p < .0001$). At a point 3cm laterally, MT was 15.38 ± .22 Hz ($p < .0001$). MT at rostral points 1 and 3cm away from the reference point were 20.26 ± .79 Hz ($p = .0004$) and 18.42 ± .33 Hz ($p = .99$), respectively. Lastly, at a point 1cm caudally away from the reference point, MT was 20.40 ± .35 Hz (.0002). At a point 3cm away, MT was 18.76 ± .38 Hz ($p = .807$).

Similar data were also collected for ME at these differing points. These data were then compared to the reference point for statistical significance ($p < .05$, Figure 9). At the reference point, mean ME was 1.47 ± .026. At a point 1cm laterally, ME was 1.64 ± .034 ($p < .0001$). At a point 3cm laterally, ME was .91 ± .02 ($p < .0001$). ME at rostral points 1 and 3cm away from the reference point were 1.34 ± .07 ($p = .0006$) and 1.59 ± .04 ($p = .0012$), respectively. Lastly, at a point 1cm caudally away from the reference point, ME was 1.56 ± .05 (.0211). At a point 3cm away, ME was 1.45 ± .05 ($p = .9$).

Lastly, we measured the deviation in MS at points laterally, rostrally, and caudally from a reference point on the PSM. The data collected at these differing points were then compared to the reference point for statistical significance ($p < .05$, Figure 10). At the reference point, mean MS was 361 ± 6.12 N/m. At a point 1cm laterally, MS was 321.6 ± 8.02 N/m ($p < .0001$). At a point 3cm laterally, MS was 261.6 ± 6.23 N/m ($p < .0001$). MS at rostral points 1 and 3cm away from the reference point were 403 ± 12.94 N/m ($p < .0001$) and 419.8 ± 7.33 N/m ($p < .0001$), respectively. Lastly, at a point 1 cm caudally away from the reference point, MS was 381.6 ± 13.79 N/m ($p = .0062$). At a point 3 cm away, MS was 343.6 ± 4.34 N/m ($p = .024$).

Qualitative comparison of ultrasound images taken across two operators both with and without the use of a belt demonstrates more consistent reflectance patterns with the aid of a guiding belt (Figure 7). Blue arrows indicate the consistent border (a region of higher reflectance) of the PSM in images taken with the belt. These borders were not able to be visualized in images taken without the belt.

6 EXPERIMENT 2

6.1 Study Design

Prior to participating, the subject was informed of the procedures, risks, and purpose of the study. The subject began by removing any articles of clothing on their upper body. A ButterflyIQ ultrasound was then used to measure subcutaneous fat thickness at the forearm, chest, upper abdominals, lower abdominals, lateral abdominals, and shoulder (Figure 11). A musculoskeletal ultrasound preset was used and a visualization depth of 3 cm was kept constant throughout the experiment. Subcutaneous fat thickness was determined through utilization of a line measurement function at the center of the ultrasound image in the ButterflyIQ visualization program. Care was taken not to apply too much pressure so as to avoid compression of the subcutaneous fat layer. Tissue was determined to be subcutaneous fat based on its higher reflectance, location relative to the dermis, and absence of visualized muscle fibers that were present in the underlying muscle. Immediately following Ultrasound measurements, MYOTON data was collected at each anatomical location in both fully relaxed and full isometric contraction states. The level of isometric contraction was determined via the Borg Rating of Perceived Exertion (Hampton et al, 2014).

Differences between relaxed contracted states for each biomarker were then compared and tested for statistical significance. Since each region had a different thickness of subcutaneous fat, the degree of statistical significance between relaxed and contracted states (p-values) were plotted against their respective subcutaneous fat thicknesses. A nonlinear quadratic regression model was then applied to the data to predict the extent to which the thickness of the subcutaneous fat layer affects detection of differences in muscular biomarkers in MYOTON measurements.

6.2 Results

Mean subcutaneous fat thickness was .30 ± .04 cm at the forearm, .57 ± .05 cm at the chest, 1.25 ± .12 cm at the upper abdominals, 1.16 ± .13 cm at the lower abdominals, .73 ± .05 cm at the lateral abdominals, .18 ± .02 cm at the bicep, and .29 ± .03 cm at the shoulder (Table 1, Table2, Table 3).

For MT, values in the relaxed state were 16.92 ± .61 Hz at the forearm, 11.93 ± .89 Hz at the chest, 11.99 ± .62 Hz at the upper abdominals, 11.55 ± .37 at the lower abdominals, 12.63 ± .22 Hz at the lateral abdominals, 14.97 ± 1.16 Hz at the bicep, and 14.03 ± .38 Hz at the shoulder (Table 1). In the full isometric contraction state, values for MT were 21.8 ± 2.44 Hz at the forearm, 17.27 ±1.25 Hz at the chest, 11.85 ± .76 Hz at the upper abdominals, 11.18 ± .44 Hz at the lower abdominals, 14.18 ± 1.06 Hz at the lateral abdominals, 20.65 ± .92 Hz at the bicep, and 21.25 ± 1.65 Hz at the shoulder (Table 1). Delta values detecting a statistically significant difference between relaxed and contracted states were 4.88 Hz for the forearm ($p = .0028$), 5.33 Hz for the chest ($p = .0015$), -.15 Hz for the upper abdominals ($p = .472$), -.37 Hz for the lower abdominals ($p = .17$), 1.55 Hz for the lateral abdominals ($p = .026$), 5.68 Hz for the Bicep ($p < .0001$), and 7.22 Hz for the shoulder ($p < .0001$, Table 1).

For ME, values in the relaxed state were .87 ± .04 at the forearm, 1.18 ± .14 at the chest, 1.48 ± .10 at the upper abdominals, 1.23 ± .06 at the lower abdominals, 1.097 ± .05 at the lateral abdominals, 1.13 ± .07 at the bicep, and 1.06 ± .14 at the shoulder (Table 2). In the full isometric contraction state, values for ME were .87 ± .09 at the forearm, 1.05 ± .097 at the chest, 1.38 ± .18 at the upper abdominals, 1.18 ± .04 at the lower abdominals, 1.27 ± .16 at the lateral abdominals, .75 ± .08 at the bicep, and .77 ± .07 at the shoulder (Table 2). Delta values detecting a statistically significant difference between relaxed and contracted states were 0.0 for the forearm ($p = 1$), -.12 for the chest ($p = .225$), -.10 for the upper abdominals ($p = .37$), -.035 for the lower abdominals ($p = .25$), .177 for the lateral abdominals ($p = .057$, -.38 for the Bicep ($p = .000257$), and -.29 for the shoulder ($p = .0063$, Table 2).

For MS, values in the relaxed state were 299 ± 24.3 N/m at the forearm, 183.8 ± 23.4 N/m at the chest, 203.5 ± 23.05 N/m at the upper abdominals, 126.8 ± 61.97 N/m at the lower abdominals, 185.67 ± 8.04 N/m at the lateral abdominals, 226.2 ± 17.1 N/m at the bicep, and 223.67 ± 4.8 N/m at the shoulder (Table 3). In the full isometric contraction state, values for MS were 542.8 ± 98.3 N/m at the forearm, 465.5 ± 74.4 N/m at the chest, 191.3 ± 22.17 N/m at the upper abdominals, 144.17 ± 9.6 N/m at the lower abdominals, 269.0 ± 59.7 N/m at the lateral abdominals, 408.5 ± 35.6 N/m at the bicep, and 505.8 ± 89.3 N/m at the shoulder (Table 3). Delta values detecting a statistically significant difference between relaxed and contracted states were 243.8 N/m for the forearm ($p = .0013$), 281.7 N/m for the chest ($p = .00058$), -12.2 N/m for the upper abdominals ($p = .03$), 17.4 N/m for the lower abdominals ($p = .54$), 83.3 N/m for the lateral abdominals ($p = .021$), 182.3 N/m for the Bicep ($p < .0001$), and 282.2 Nm for the shoulder ($p = .0006$, Table 3).

The thickness of the subcutaneous fat of each region were plotted against their corresponding p-value detecting if there is a statistically significant difference between relaxed and contracted states. These data were then used to generate a quadratic regression model (Figure 12, Figure 13, Figure 14). Plugging in the desired output p-value of .05 (threshold of statistical significance) into these regression models allowed us to predict the maximum subcutaneous fat thickness before detection of changes in MYOTON data become confounded. For the MT regression model, using $p = .05$ as an output yielded a fat thickness of .73 cm. For the ME regression model, using $p = .05$ as an output yielded a fat thickness of .67 cm. And for the MS regression model, using $p = .05$ as an output yielded a fat thickness of .668 cm. Averaging these values together, our model predicts that .689 ± .035 cm is the maximum thickness of subcutaneous fat before MYOTON data becomes confounded and unreliable.

7 EXPERIMENT 3

7.1 Study Design

Prior to participating, the subject was informed of the procedures, risks, and purpose of the study. To test for the extent to which resistance exercise affects MYOTON biomarker data, baseline measurements of MT, MS, and ME were taken at a marked region of the chest. The subject then performed a series of 100 push-ups as two sets of 50. Immediately following this exercise, MYOTON data was collected at 2-minute intervals for 10 minutes after the conclusion of the push-ups. As a controlled trial, the same protocol was performed without performing push-ups beforehand. These data were then plotted to observe the extent to which resistance exercise can confound MYOTON data measurements.

7.2 Results

For MT, values increased to 12.55 ± .44 Hz immediately post-exercise and returned to baseline within the 10 minute timespan allocated for measurements (Figure 15). For ME, no changes were detected post exercise (Figure 16). For MS, values increased to 170.67 ± 6.22 N/m immediately post-exercise and returned to baseline within the 10 minute timespan allocated for measurements (Figure 17).

8 GENERAL DISCUSSION

To our knowledge, this study was the first to evaluate a means of consistent muscular biomarker data collection on the PSM. Additionally, we were the first to observe the extent to which subcutaneous fat thickness and exercise can confound MYOTON data.

Regarding our first experiment, we conclude that the use of a guiding belt improves data reliability and accuracy when compared to MYOTON data collected without a guiding belt. For MT, we observed a statistically significant increase in MT values taken with the belt than those taken without (Figure 1). This is indicative that the guiding belt we designed is allowing for improved accuracy of measurements taken on more appropriate regions of the PSM. This is further supported by our observation that MT decreases significantly as one moves laterally away from a reference location on the PSM, indicating that measurements taken without the belt were most likely lateral to the desired loci on the PSM (Figure 8).

We observed a decrease in standard deviations for MT measurements with the use of the belt, however, this difference was not statistically significant (Figure 2). We postulate that this is due to the vertical muscular homogeneity of the PSM (Willard et al, 2012). Additionally, MYOTON data collected at 3cm rostrally and caudally were not statistically significant when compared to MT data at a set reference point (figure 8). This indicates that differentiation in MT values on the vertical axis of the muscle will be less pronounced than those on the lateral axis, potentially reducing the spread of data taken without the guiding belt. Furthermore, provided COVID-19 restrictions are no longer in place, increasing the number of subjects enrolled in future studies may resolve this issue. Taken together, these data on MT allow us to conclude that our guiding belt improves data reliability by guiding operators to a more consistent and appropriate region on the PSM.

For ME, we observed a statistically significant decrease in ME values taken with a guiding belt than data taken without (Figure 1). As stated with our data on MT, this is indicative that the guiding belt we designed is allowing for improved accuracy of measurements taken on more appropriate regions of the

PSM. This is supported by our observation that ME increases significantly as one moves 1cm laterally away from a reference location on the PSM (Figure 8).

In addition, we observed a statistically significant decrease in standard deviations in ME measurements with the use of the belt when compared to those from data taken without a guiding belt (Figure 4). This supports our hypothesis that our guiding belt reduces the spread of MYOTON data. These results on ME allow us to conclude that our guiding belt effectively reduces the standard deviation of ME measurements in addition to guiding operators to a more appropriate region on the PSM for measurement.

Lastly, we observed a statistically significant increase in MS values taken with the belt than those taken without (Figure 5). This indicates that the guiding belt we designed improves accuracy of MYOTON biomarker data by allowing for measurements on more appropriate regions of the PSM. Additionally, this supported by our observation that MS decreases significantly as one moves both 1cm and 3cm laterally away from a reference location on the PSM (Figure 10).

We observed a decrease in standard deviations for MS measurements with the use of the belt, however, this difference was not statistically significant (Figure 6). As stated in our analysis for MT, we believe that this is due to the vertical muscular homogeneity of the PSM (Willard et al, 2012). Data collected at points rostrally away from a set reference point did have statistically significant increases in MS values when compared reference point data. However, MS values at caudal loci had less pronounced differences. Because MS has less differentiation on the vertical axis than on the lateral one, this could potentially reduce the spread of data taken without the guiding belt, as we observed in our experiment. Additionally, because we were limited to only one subject, it is possible that increasing the number of subjects will resolve this issue. Taken together, these data on MT allow us to conclude that our guiding belt improves data reliability by guiding operators to a more consistent and appropriate region of the PSM.

Per request of the French Space Agency, an additional housing for a remotely controlled ultrasound was added to our guiding belt. This will allow for a professional sonographer to collect spaceflight data

on astronauts from Earth (Arbeille et al, 2018; Garcia et al 2018; Arbeille et al, 2016). Because we did not have access to this device, we wanted to validate that this guiding belt improves PSM image consistency. To test this, images were taken both with and without the belt across two different operators. Qualitative analysis of reflectance patterns indicates that our guiding belt improves image consistency. More specifically, a region of high reflectance representing the border of the PSM was consistently visualized in images taken with the belt. We were unable to visualize this anatomical landmark in images taken without the belt (figure 7). These qualitative results allow us to conclude that ultrasound image consistency is improved with the use of a guiding belt.

Taken together, the results of our first experiment support the hypothesis that our guiding belt improves MYOTON and ultrasound data reliability and accuracy. We propose that this belt will allow for accurate and efficient monitoring of muscular biomarkers in future space missions. Furthermore, the protocol developed in experiment will be implemented in a larger Preventative Medical Ultrasound (PMU) study in collaboration with NASA, the European Space Agency (ESA), and the French Space Agency (CNES).

For our second experiment, we wanted to evaluate the extent to which subcutaneous fat thickness affects detection of changes in MYOTON muscular biomarker data. We plotted the thicknesses of subcutaneous fat layers at multiple anatomical loci against the p-values detecting statistically significant changes in MYOTON data between relaxed and isometrically contracted states. In doing so, we were able to apply a quadratic regression model to each biofactor to predict the maximum thickness of subcutaneous fat before MYOTON data become confounded and are no longer valid (figure 12, figure 13, figure 14). We concluded that $.689 \pm .035$ cm is this maximum thickness. However, it is important to note that this solely serves the purpose of establishing a protocol for future experiments. We believe that including more subjects in this study will improve this model and yield results more representative of the general population.

Since the MYOTON probe has uses both in space medicine and medicine on earth, conclusions drawn in this study may be applied as an exclusion factor for medical use of this device (Agyapong-Badu

et al, 2021; Berzosa et al, 2021; Milerska et al, 2020; Garcia-Bernal et al, 2021). Examination of subcutaneous fat thickness at a specific region prior to MYOTON measurements may determine its degree of confidence as an accurate evaluation of muscular biomarkers. This may help guide and improve future clinical decisions both on Earth and in Space. Regarding future spaceflight studies using this device, it may be necessary to measure subcutaneous fat thickness at specific regions in candidate astronauts. This may serve as an exclusion factor to participate in the study. Furthermore, for those individuals who have greater subcutaneous fat thicknesses, ultrasound screening can be performed to find loci whose subcutaneous fat thickness is low enough where it won't confound MYOTON data. Since astronauts' body compositions may change over time, tracking subcutaneous fat thickness may also be necessary in long term studies.

Lastly, our third experiment aimed to determine if resistance exercise can confound MYOTON data should it be collected after its completion. Since astronauts undergo a strict physical training regime to prevent physiological deconditioning (James A et al, 2015), determining if this can affect MYOTON data was deemed necessary. Our data indicated that there was an immediate increase in MT and MS biofactors in the minutes following completion of a 100 push-up exercise protocol (Figure 15, figure 17). ME was not affected by exercise (Figure 16). For MT and MS, the effect of exercise was short lasting, and values returned to baseline within the 10 minute timespan of the study. This increase in MT and MS was likely due to local increases in blood flow commonly observed during exercise (Laughlin et al, 1999). Once exercise was completed and the subject was allowed to rest, local blood flow redistributed, allowing for MT and MS to return to baseline values.

These results indicate that resistance exercise can confound MYOTON data should it be collected in close proximity to the completion of training. However, it is important to note the significant limitations of this experiment. MYOTON data was only collected at one muscle group. Thus, we cannot draw broad conclusions based on our results. Rather, our data can only be applied to the pectoral muscle group in relation to resistance exercise involving these muscles. Additionally, it is possible that whole body exercise may have more pronounced effects on MYOTON data than solely exercising one muscle group.

Delayed onset muscle soreness due to ultrastructural muscle damage of myofibrils has been shown to increase muscle stiffness and cause local inflammation, and this may affect MYOTON data (Hotfiel et al, 2018). Since astronauts' training regime is traditionally resistance exercise heavy (James et al, 2015), studying the effects of whole-body exercise on MYOTON data may be worth future study.

In conclusion, this study evaluated the use of a MYOTON probe as a means for spaceflight monitoring of muscular biomarkers. To improve the reliability and accuracy of data collected from the PSM, we designed and validated a MYOTON and ultrasound guiding belt. It was demonstrated that this guiding belt improves the reliability and accuracy of MYOTON data across multiple operators. Additionally, we established a protocol and collected preliminary data on the extent to which subcutaneous fat can confound MYOTON detection of changes in muscular biomarkers. Lastly, we evaluated the effects that single muscle resistance exercise has on MYOTON data. While this study was primarily focused on spaceflight medicine, our results can be applied to contexts of medicine and sports science. These experiments serve to further human progress in spaceflight by allowing for effective monitoring of muscular biomarkers in future missions to Mars and beyond.

Limitations and Future Considerations

As previously stated, the most significant limitation of this study was our restriction to only collecting data on one subject. While we attempted to mitigate this issue by performing repeated trials on this subject, this limitation prevents us from extrapolating our conclusions to the general population. As a result, this study should be treated as laying the groundwork for future studies. More specifically, inclusion of more data points in our quadratic regression model will improve its accuracy in predicting the limit of subcutaneous fat thickness. This would permit extrapolation of the model to the general population, improving the MYOTON's use in medical applications.

In addition to including more subjects in the exercise portion of this study, it would be worthwhile to include trials involving whole body exercise, training involving multiple muscle groups, and cardiovascular exercise. Results from such experiments would provide a more complete evaluation of

the effects of exercise on MYOTON data collection. Since exercise is the primary countermeasure for muscular deconditioning (James et al, 2015), studies involving multiple experimental groups performing different forms of exercise may allow for optimization of a training regime to prevent muscular deconditioning in long term spaceflight.

Lastly, our MYOTON and ultrasound guiding belt is planned for use in a NASA integrated mission project. We are 1 of 14 teams that will coordinate our project into a single cohesive package of protocols that will be offered to a total of 30 astronauts. In addition to MYOTON monitoring of muscular biomarkers, our specific project will focus on ultrasounds of the organs/vessels that could be affected during long term spaceflight. This includes the superficial and deep soft organs and vessels, (Intra cranial, Carotid, Jugular, leg vessels, thyroid, neck leg muscle, Achille tendon, heart, Liver, pancreas, kidney, pelvic organs) as well as the neck and lumbar muscle/disc/vertebra unit. This ultrasound investigation will be tele-operated from the ground in order to reduce preflight training and astronaut workload.

Despite the limitations of our study, our experiments further progress in human spaceflight research. The results and protocols garnered from this study will hopefully lead to safer and more effective space travel in the future.

9 APPENDIX

9.1 Tables

Table 1: Table of differences in muscular tone (Hz) measured by a MYOTON between relaxed and full isometric contraction states. Fat thickness was measured via a line function in the ButterflyIQ visualization system. Δ-value indicates the difference in muscle tone between relaxed and contracted states. The p-value column indicates whether the Δ-value is a statistically significant difference.

Difference in Muscular Tone Between Relaxed and Contracted States

Location	Fat thickness (cm)	Relaxed tone (Hz)	Contracted tone (Hz)	Δ-value	p-value
Forearm	.30 ± .04	16.92 ± .61	21.8 ± 2.44	4.88	.0028*
Chest	.57 ± .05	11.93 ± .89	17.27 ±1.25	5.33	.0015*
Upper abdominals	1.25 ± .12	11.99 ± .62	11.85 ± .76	-.15	.472
Lower abdominals	1.16 ± .13	11.55 ± .37	11.18 ± .44	-.37	.17
Lateral abdominals	.73 ± .05	12.63 ± .22	14.18 ± 1.06	1.55	.026*
Bicep	.18 ± .02	14.97 ± 1.16	20.65 ± .92	5.68	9.23E - 06*
Shoulder	.29 ± .03	14.03 ± .38	21.25 ± 1.65	7.22	9.85E - 05*

* Indicates Δ-value is a statistically significant difference ($p < .05$)

Table 2: Table of differences in muscular elasticity (log decrement) measured by a MYOTON between relaxed and full isometric contraction states. Fat thickness was measured via a line function in the ButterflyIQ visualization system. Δ-value indicates the difference in muscle tone between relaxed and contracted states. The p-value column indicates whether the Δ-value is a statistically significant difference.

Difference in Muscular Elasticity Between Relaxed and Contracted States

Location	Fat thickness (cm)	Relaxed elasticity (Log decrement)	Contracted elasticity (Log decrement)	Δ-value	p-value
Forearm	.30 ± .04	.87 ± .04	.87 ± .09	0	1
Chest	.57 ± .05	1.18 ± .14	1.05 ± .097	-.12	.225
Upper abdominals	1.25 ± .12	1.48 ± .10	1.38 ± .18	-.10	.37
Lower abdominals	1.16 ± .13	1.23 ± .06	1.18 ± .04	-.035	.25
Lateral abdominals	.73 ± .05	1.097 ± .05	1.27 ± .16	.177	.057
Bicep	.18 ± .02	1.13 ± .07	.75 ± .08	-.38	.000257*
Shoulder	.29 ± .03	1.06 ± .14	.77 ± .07	-.29	.0063*

* Indicates Δ-value is a statistically significant difference ($p < .05$)

Table 3: Table of differences in muscular stiffness (N/m) measured by a MYOTON between relaxed and full isometric contraction states. Fat thickness was measured via a line function in the ButterflyIQ visualization system. Δ-value indicates the difference in muscle tone between relaxed and contracted states. The p-value column indicates whether the Δ-value is a statistically significant difference.

Difference in Muscular Stiffness Between Relaxed and Contracted States

Location	Fat thickness (cm)	Relaxed Stiffness (N/m)	Contracted Stiffness (N/m)	Δ-value	p-value
Forearm	.30 ± .04	299 ± 24.3	542.8 ± 98.3	243.8	.0013*
Chest	.57 ± .05	183.8 ± 23.4	465.5 ± 74.4	281.7	.00058*
Upper abdominals	1.25 ± .12	203.5 ± 23.05	191.3 ± 22.17	-12.2	.03*
Lower abdominals	1.16 ± .13	126.8 ± 61.97	144.17 ± 9.6	17.4	.54
Lateral abdominals	.73 ± .05	185.67 ± 8.04	269.0 ± 59.7	83.3	.021*
Bicep	.18 ± .02	226.2 ± 17.1	408.5 ± 35.6	182.3	2.12E - 05*
Shoulder	.29 ± .03	223.67 ± 4.8	505.8 ± 89.3	282.2	.0006*

* Indicates Δ-value is a statistically significant difference ($p < .05$)

9.2 Figures

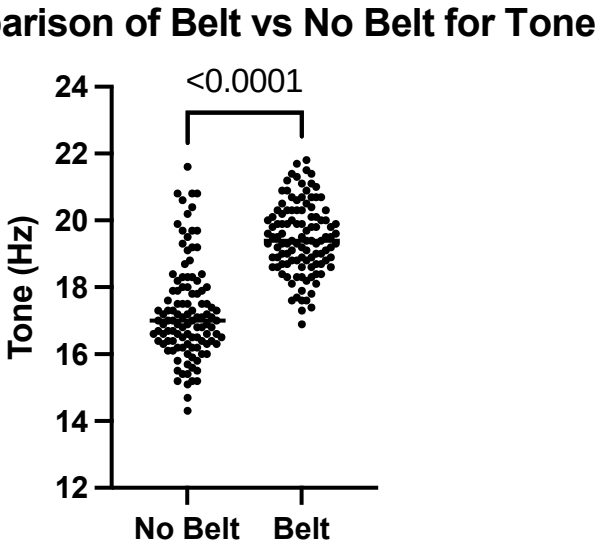

Figure 1: A comparison of measurements in muscle tone taken with a MYOTON probe both with and without the use of a guiding belt. Multiple operators were used in the collection of these data. A p-value < .05 denotes a statistically significant difference.

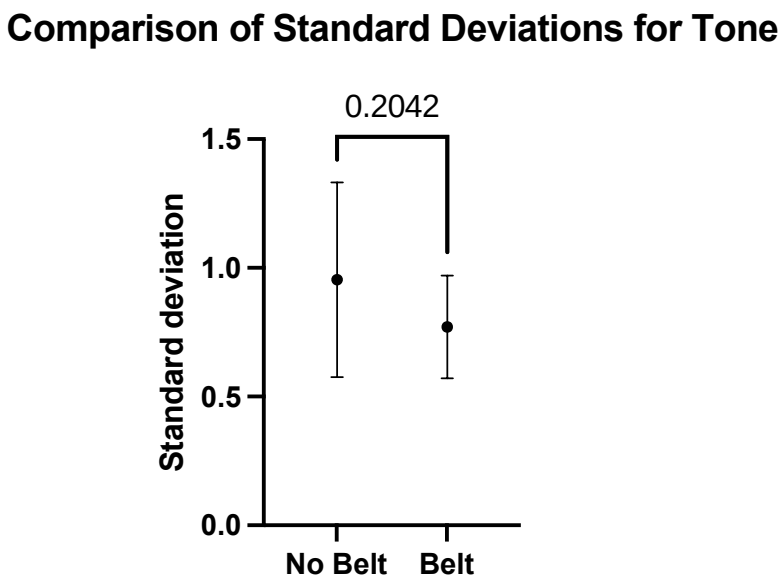

Figure 2: A comparison of aggregated standard deviations from each trial (N = 12) of muscle tone measurements taken with a MYOTON probe both with and without the use of a guiding belt. Multiple operators were used in the collection of these data. A p-value < .05 denotes a statistically significant difference.

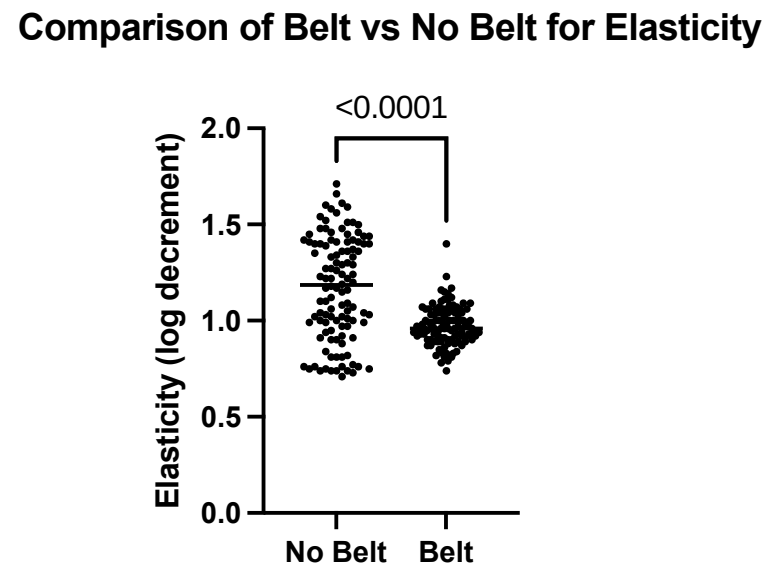

Figure 3: A comparison of measurements in muscle elasticity taken with a MYOTON probe both with and without the use of a guiding belt. Multiple operators were used in the collection of these data. A p-value < .05 denotes a statistically significant difference.

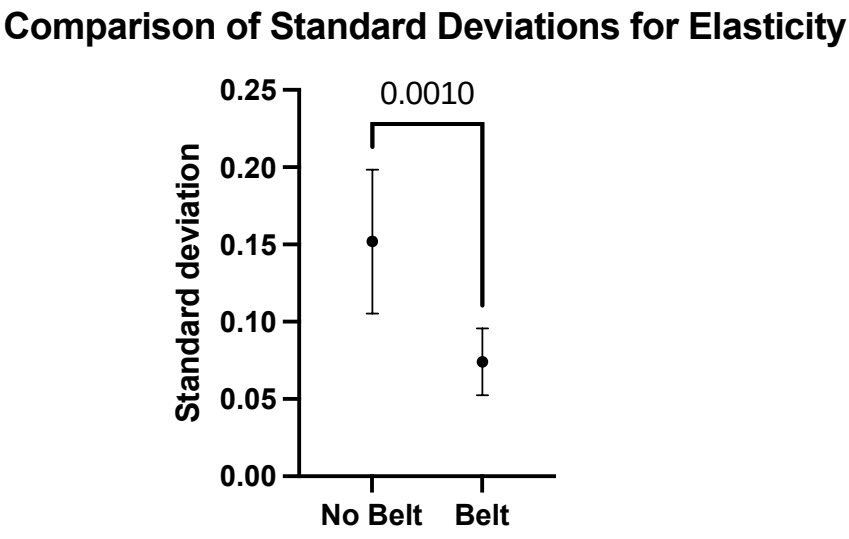

Figure 4: A comparison of aggregated standard deviations from each trial (N = 12) of muscle elasticity measurements taken with a MYOTON probe both with and without the use of a guiding belt. Multiple operators were used in the collection of these data. A p-value < .05 denotes a statistically significant difference.

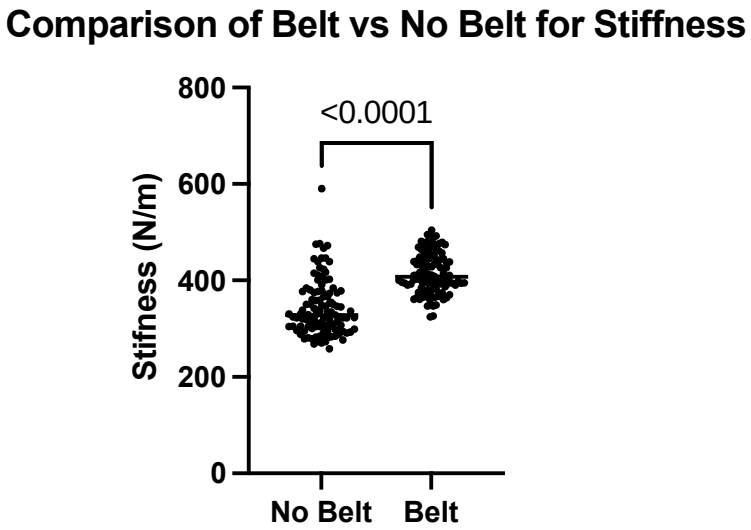

Figure 5: A comparison of measurements in muscle stiffness taken with a MYOTON probe both with and without the use of a guiding belt. Multiple operators were used in the collection of these data. A p-value < .05 denotes a statistically significant difference.

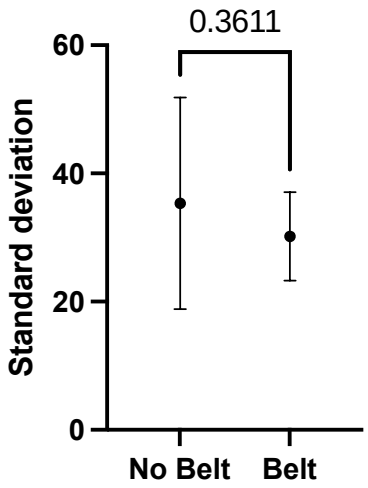

Figure 6: A comparison of aggregated standard deviations from each trial (N = 12) of muscle stiffness measurements taken with a MYOTON probe both with and without the use of a guiding belt. Multiple operators were used in the collection of these data. A p-value < .05 denotes a statistically significant difference.

No Belt **Belt**

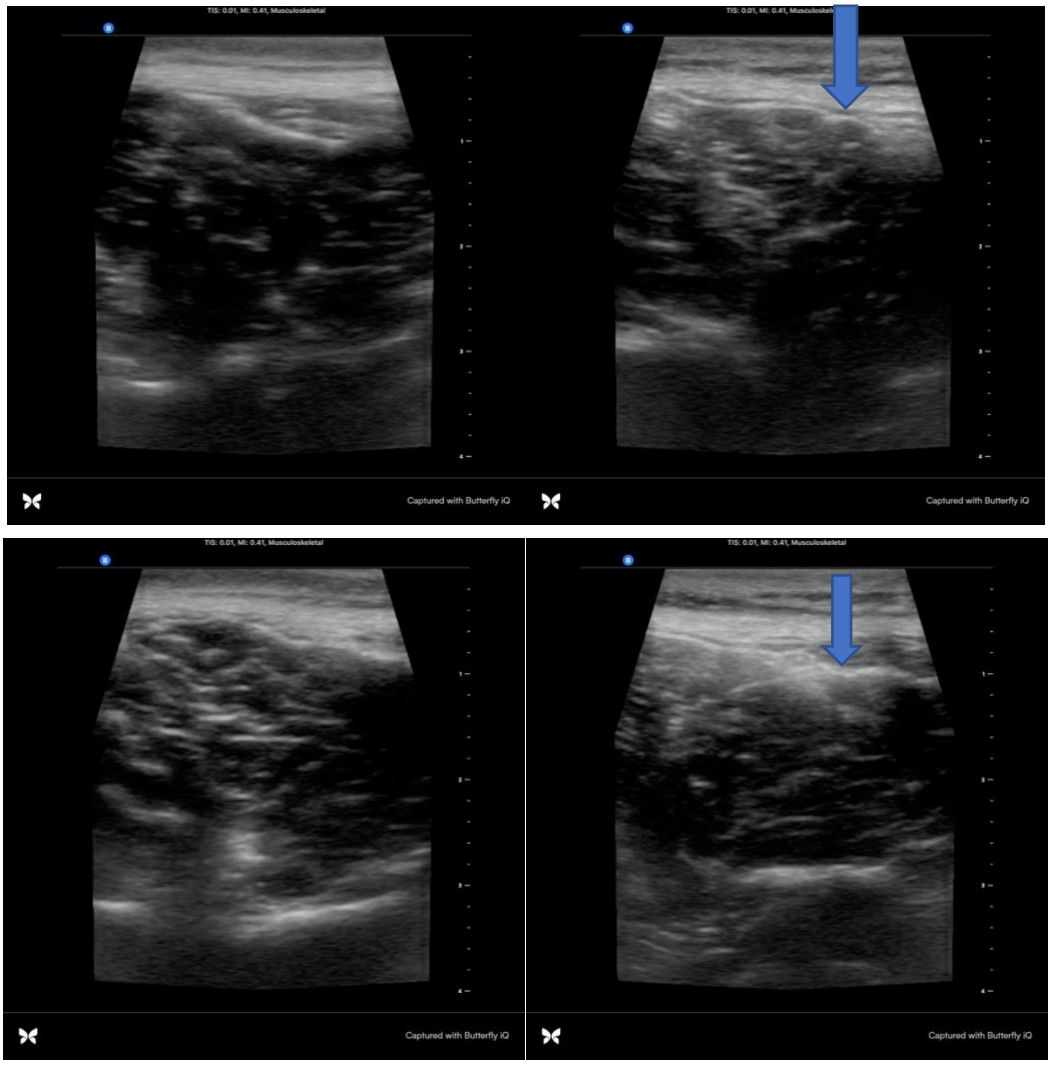

Figure 7: A qualitative comparison of screen captured ultrasound images taken with a ButterflyIQ ultrasound. Both sets of images were taken with two different operators. Left: visualization of the PSM without the belt. Right: visualization with the use of a guiding belt. Qualitative comparison of the two groups demonstrates more consistent reflectance patterns across multiple operators with the aid of a guiding belt. Blue arrows indicate the consistent border of the PSM in images taken with the belt. These borders were not able to be visualized in images taken without the belt.

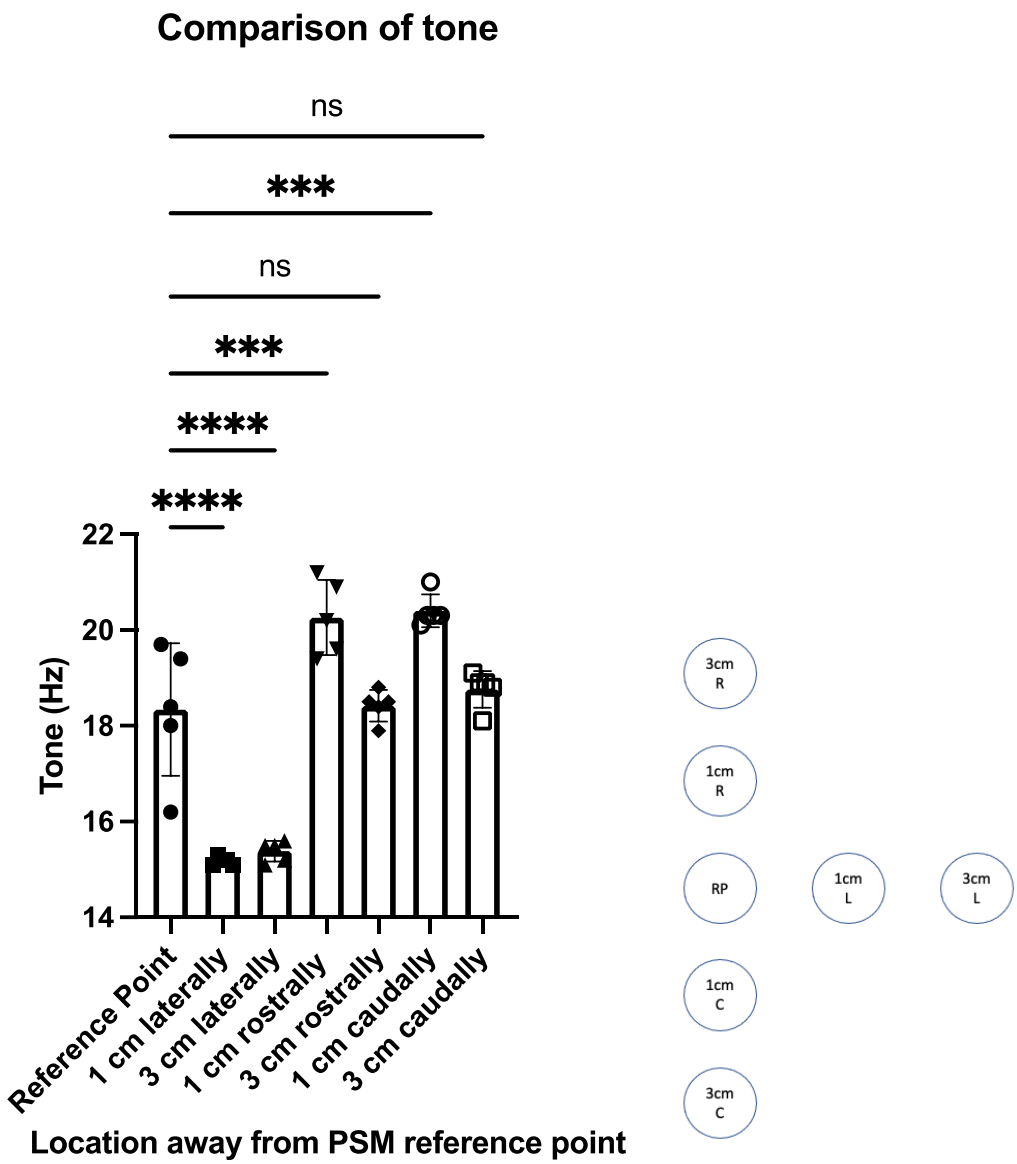

Figure 8a (left): Muscle tone data collected with a MYOTON probe at a specified anatomical reference point at the center of a paraspinal muscle (PSM). Subsequent measurements were taken at points laterally, rostrally, and caudally away from the specified reference point. All loci were marked with a pen before data collection. An ordinary 1-way ANOVA test was done to compare these data to that of the original reference point. Figure 8b (right): Spatial pattern for collection of MYOTON data. RP = reference point; R = rostral points; C = caudal points; L = lateral points.

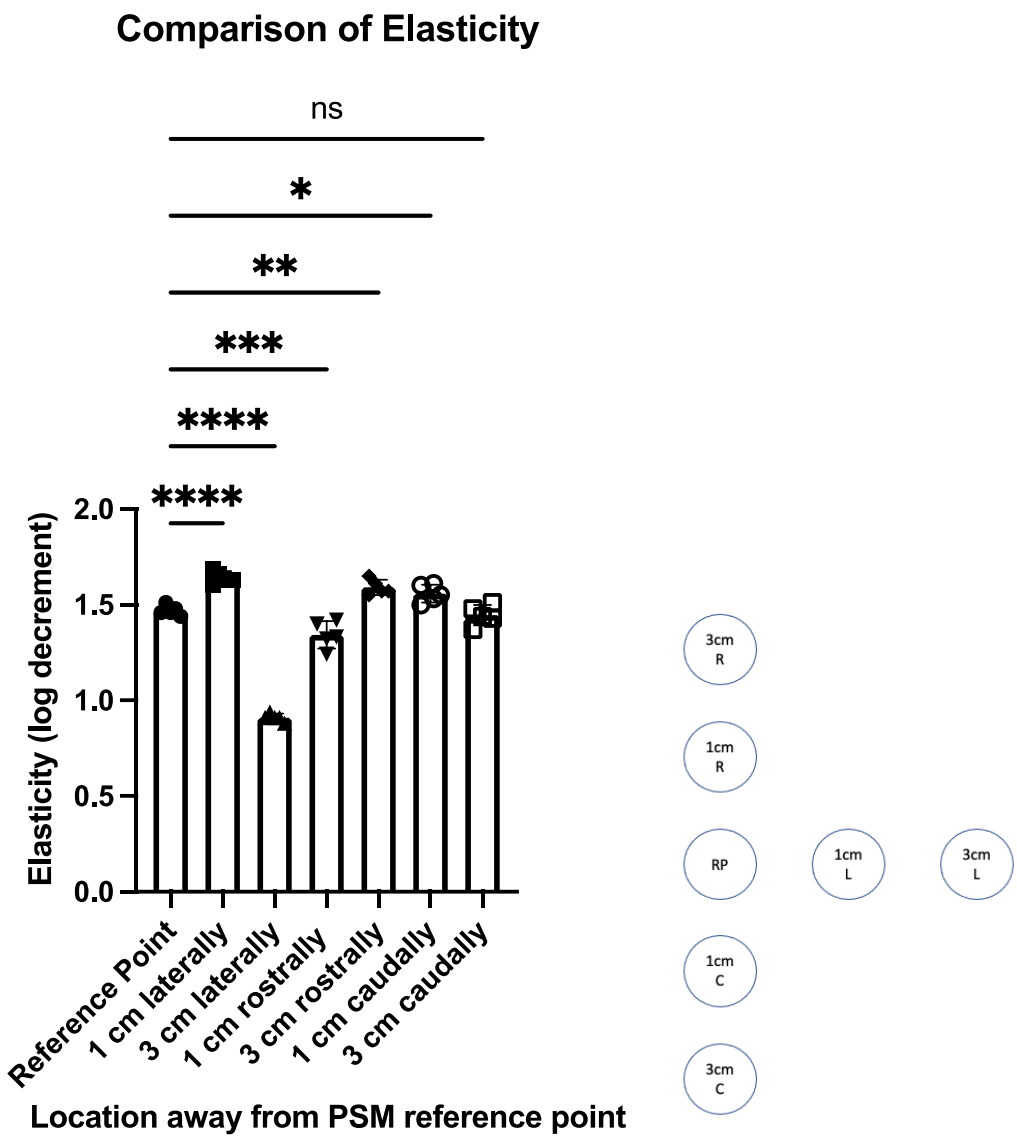

Figure 9a (left): Muscle elasticity data collected with a MYOTON probe at a specified anatomical reference point at the center of a paraspinal muscle (PSM). Subsequent measurements were taken at points laterally, rostrally, and caudally away from the specified reference point. All loci were marked with a pen before data collection. An ordinary 1-way ANOVA test was done to compare these data to that of the original reference point. Figure 9b (right): Spatial pattern for collection of MYOTON data. RP = reference point; R = rostral points; C = caudal points; L = lateral points.

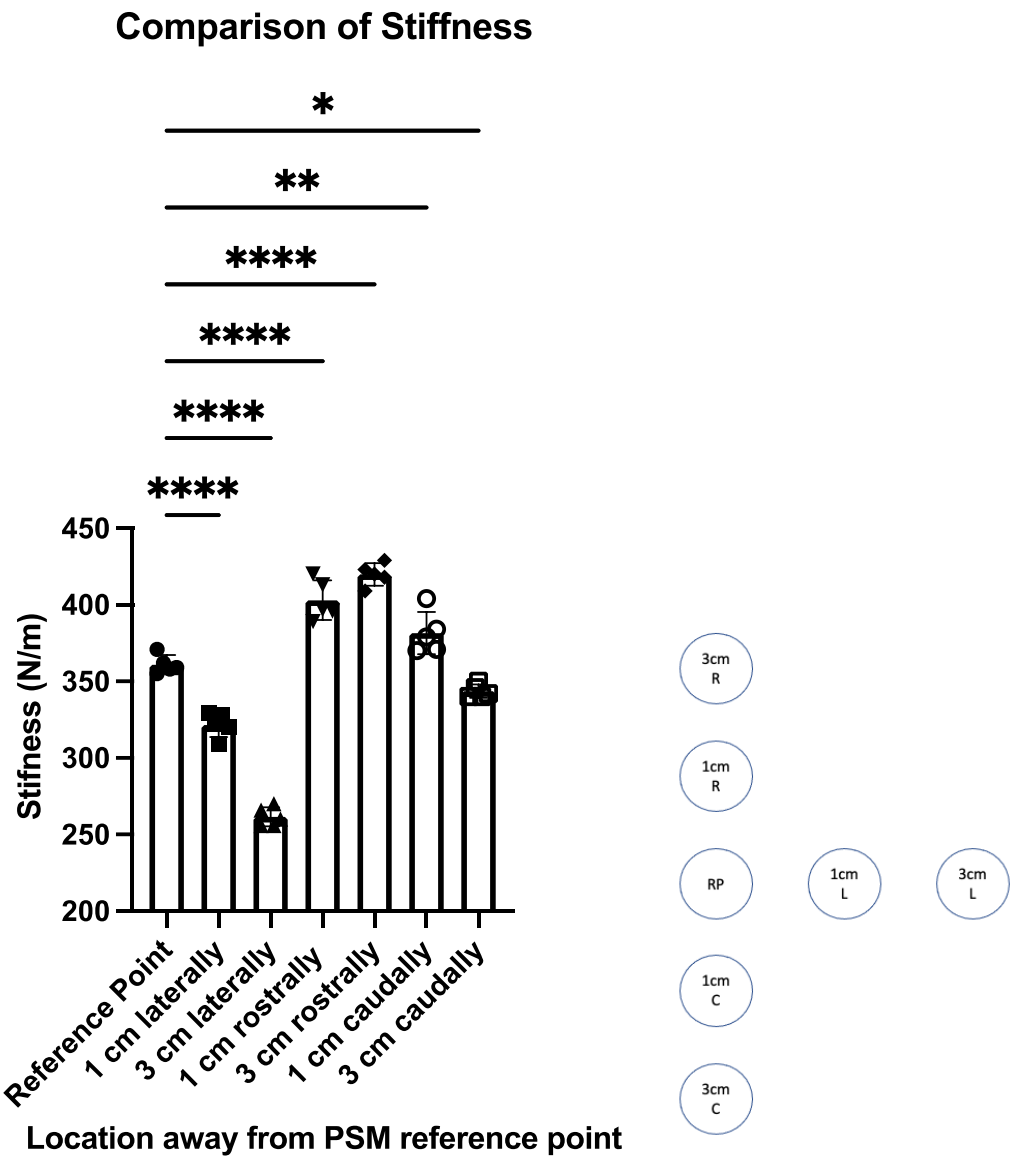

Figure 10a (left): Muscle stiffness data collected with a MYOTON probe at a specified anatomical reference point at the center of a paraspinal muscle **(PSM)**. Subsequent measurements were taken at points laterally, rostrally, and caudally away from the specified reference point. All loci were marked with a pen before data collection. An ordinary 1-way ANOVA test was done to compare these data to that of the original reference point. Figure 10b (right): Spatial pattern for collection of MYOTON data. RP = reference point; R = rostral points; C = caudal points; L = lateral points.

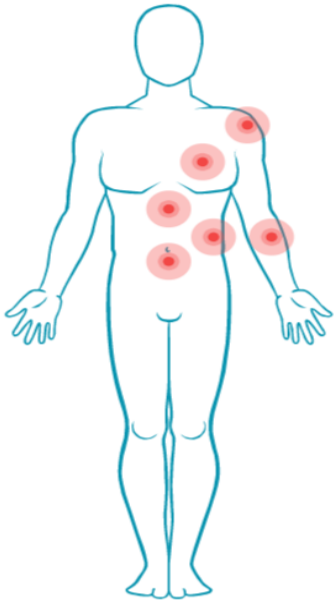

Figure 11: Spatial diagram of anatomical loci at which MYOTON and ultrasound data were collected for experiment 2. Loci are demarcated with red circles.

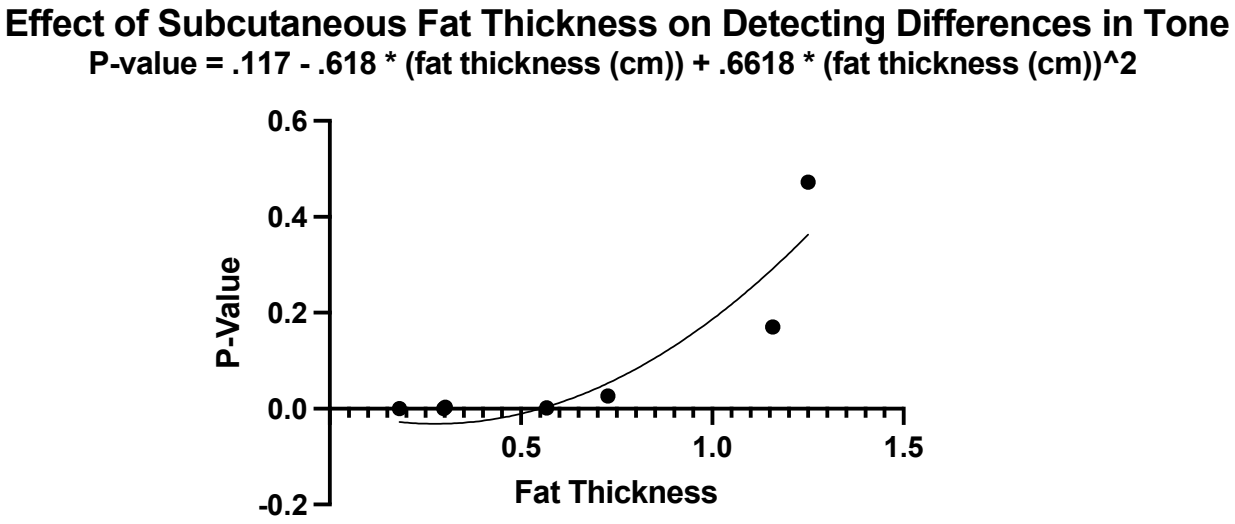

Figure 12: The effect of subcutaneous fat thickness on detecting statistically significant changes in muscle tone with a MYOTON probe between relaxed and full isometric contraction states. Varying thicknesses of subcutaneous fat imaged with a ButterflyIQ ultrasound were plotted on the x-axis. These values were plotted against the p-values detecting if there was a statistically significant difference in muscle tone between relaxed and contracted states (Δ-value, see table 1). A quadratic regression line was then plotted using the data points provided.

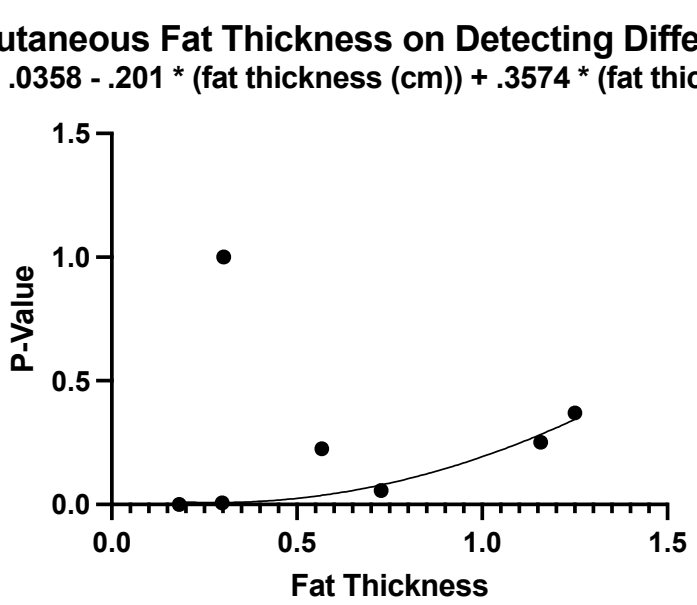

* P-value at 1 was excluded as an outlier for the regression model.

Figure 13: The effect of subcutaneous fat thickness on detecting statistically significant changes in muscle elasticity with a MYOTON probe between relaxed and full isometric contraction states. Varying thicknesses of subcutaneous fat imaged with a ButterflyIQ ultrasound were plotted on the x-axis. These values were plotted against the p-values detecting if there was a statistically significant difference in muscle elasticity between relaxed and contracted states (Δ-value, see table 1). A quadratic regression line was then plotted using the data points provided.

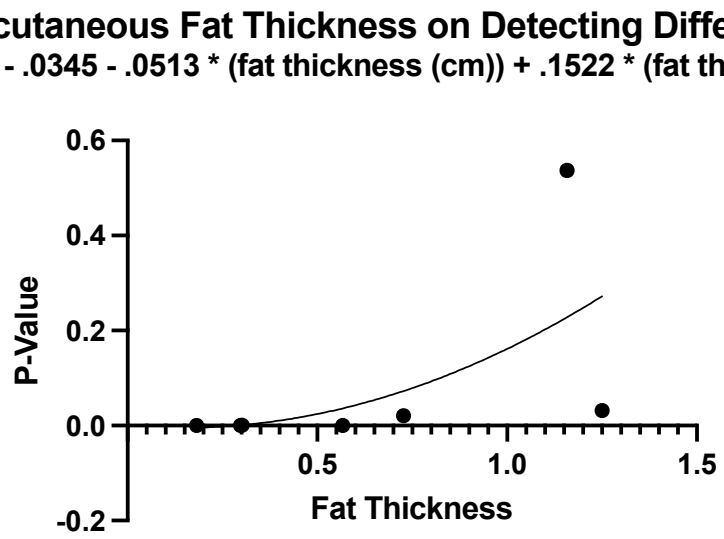

Figure 14: The effect of subcutaneous fat thickness on detecting statistically significant changes in muscle stiffness with a MYOTON probe between relaxed and full isometric contraction states. Varying thicknesses of subcutaneous fat imaged with a ButterflyIQ ultrasound were plotted on the x-axis. These values were plotted against the p-values detecting if there was a statistically significant difference in muscle stiffness between relaxed and contracted states (Δ-value, see table 1). A quadratic regression line was then plotted using the data points provided.

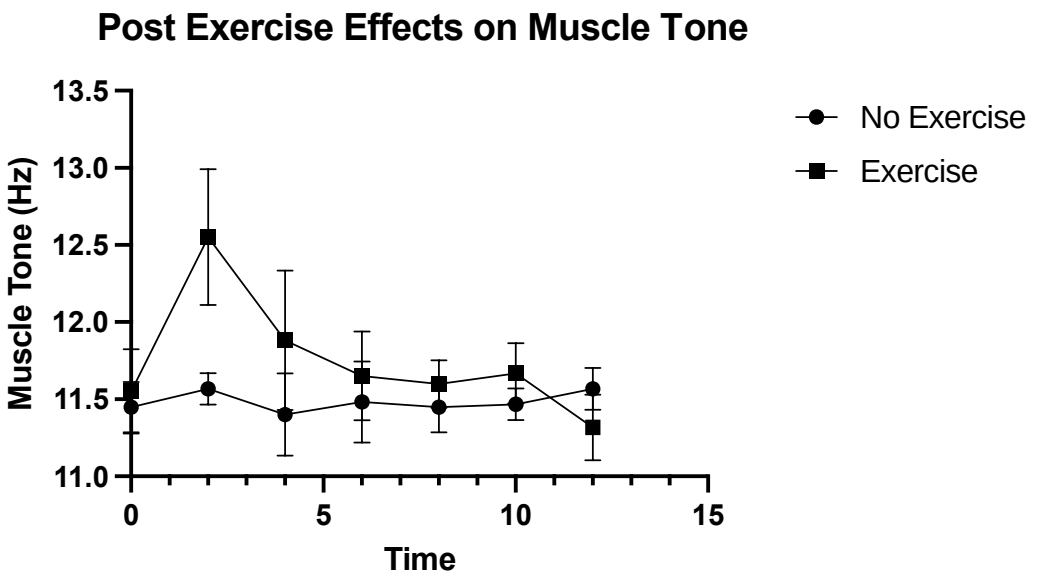

Figure 15: Post exercise effects on MYOTON muscle tone measurements. Time at 0 represents the baseline value. Measurements taken at 2 minute intervals post-exercise begin at t = 2.

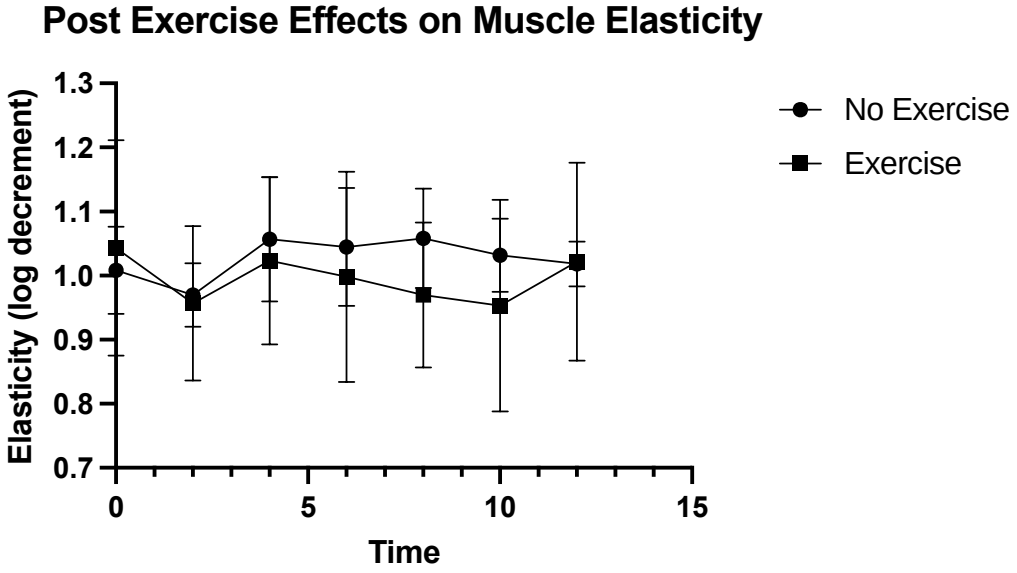

Figure 16: Post exercise effects on MYOTON muscle elasticity measurements. Time at 0 represents the baseline value. Measurements taken at 2 minute intervals post-exercise begin at t = 2.

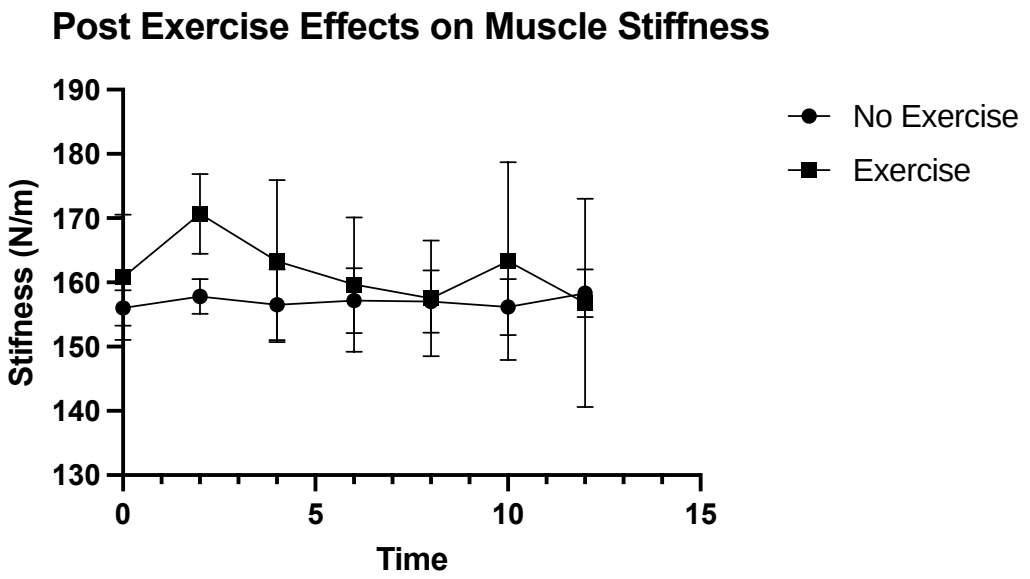

Figure 17: Post exercise effects on MYOTON muscle stiffness measurements. Time at 0 represents the baseline value. Measurements taken at 2 minute intervals post-exercise begin at t = 2.

10 REFERENCES

1. Tanaka K, Nishimura N, Kawai Y. Adaptation to microgravity, deconditioning, and countermeasures. *J Physiol Sci*. 2017;67(2):271-281. doi:10.1007/s12576-016-0514-8

2. Hotfiel T, Freiwald J, Hoppe MW, Lutter C, Forst R, Grim C, Bloch W, Hütel M, Heiss R. Advances in Delayed-Onset Muscle Soreness (DOMS): Part I: Pathogenesis and Diagnostics. *Sportverletz Sportschaden*. 2018;32(4):243-250. doi:10.1055/a-0753-1884

3. Laughlin MH. Cardiovascular response to exercise. *Am J Physiol*. 1999;277(6 Pt 2):S244-259. doi:10.1152/advances.1999.277.6.S244

4. Edgerton VR, Roy RR. Chapter 2 Neuromuscular Adaptation to Actual and Simulated Weightlessness. In: Bonting SL, ed. *Advances in Space Biology and Medicine*. Vol 4. Elsevier; 1994:33-67. doi:10.1016/S1569-2574(08)60134-3

5. Distribution of fiber types in locomotory muscles of dogs - Armstrong - 1982 - American Journal of Anatomy - Wiley Online Library. Accessed April 5, 2021. https://onlinelibrary.wiley.com/doi/abs/10.1002/aja.1001630107?casa_token=d-yDeZCimsYAAAAA:DDTP0f6nR6z2IaW96K0sq_lRuwuJNtcXG4d84CfBWZ2PYdqd3LV0nI6Ax9UrXENhiKlLmFwqs5zZ03GX

6. AKIMA, HIROSHI; KAWAKAMI, YASUO; KUBO, KEITARO; SEKIGUCHI, CHIHARU; OHSHIMA, HIROSHI; MIYAMOTO, AKIRA; FUKUNAGA, TETSUO Effect of short-duration spaceflight on thigh and leg muscle volume, Medicine & Science in Sports & Exercise: October 2000 - Volume 32 - Issue 10 - p 1743-1747

7. Baldwin KM. Effect of spaceflight on the functional, biochemical, and metabolic properties of skeletal muscle. *Medicine & Science in Sports & Exercise*. 1996;28(8):983-987.

8. D'Amelio F, Fox RA, Wu LC, Daunton NG, Corcoran ML. Effects of microgravity on muscle and cerebral cortex: a suggested interaction. *Adv Space Res*. 1998;22(2):235-244. doi:10.1016/s0273-1177(98)80015-x

9. Allen DL, Bandstra ER, Harrison BC, Thorng S, Stodieck LS, Kostenuik PJ, Morony S, Lacey DL, Hammond TG, Leinwand LL, Argraves WS, Bateman TA, Barth JL. Effects of spaceflight on murine skeletal muscle gene expression. *J Appl Physiol (1985)*. 2009;106(2):582-595. doi:10.1152/japplphysiol.90780.2008

10. Rabin R, Gordon SL, Lymn RW, Todd PW, Frey MAB, Sulzman FM. Effects of spaceflight on the musculoskeletal system: NIH and NASA future directions. *The FASEB Journal*. 1993;7(3):396-398. doi:https://doi.org/10.1096/fasebj.7.5.8462780

11. Smith JL, Edgerton VR, Betts B, Collatos TC. EMG of slow and fast ankle extensors of cat during posture, locomotion, and jumping. *Journal of Neurophysiology*. 1977;40(3):503-513. doi:10.1152/jn.1977.40.3.503

12. Stein TP, Schluter MD, Moldawer LL. Endocrine relationships during human spaceflight. *American Journal of Physiology-Endocrinology and Metabolism*. 1999;276(1):E155-E162. doi:10.1152/ajpendo.1999.276.1.E155

13. Stein TP, Leskiw MJ, Schluter MD, Hoyt RW, Lane HW, Gretebeck RE, LeBlanc AD. Energy expenditure and balance during spaceflight on the space shuttle. *American Journal of Physiology-Regulatory, Integrative and Comparative Physiology*. 1999;276(6):R1739-R1748. doi:10.1152/ajpregu.1999.276.6.R1739

14. Schneider S, Peipsi A, Stokes M, Knicker A, Abeln V. Feasibility of monitoring muscle health in microgravity environments using Myoton technology. *Med Biol Eng Comput*. 2015;53(1):57-66. doi:10.1007/s11517-014-1211-5

15. Sandri M, Sandri C, Gilbert A, Skurk C, Calabria E, Picard A, Walsh K, Schiaffino S, Lecker SH, Goldberg AL. Foxo Transcription Factors Induce the Atrophy-Related Ubiquitin Ligase Atrogin-1 and Cause Skeletal Muscle Atrophy. *Cell*. 2004;117(3):399-412. doi:10.1016/S0092-8674(04)00400-3

16. Gilman S, Arbor A. Handbook of physiology. Section 1: The nervous system, vol II. Motor control, parts 1 and 2. Section editors: John M. Brookhart and Vernon B. Mountcastle volume editor: Vernon B. Brooks Bethesda, MD, American Physiological Society, 1981 1480 pp, illustrated. *Annals of Neurology*. 1983;13(1):111-111. doi:https://doi.org/10.1002/ana.410130130

17. Milerská I, Lhotská L. Investigation of Muscle Imbalance. In: Jarm T, Cvetkoska A, Mahnič-Kalamiza S, Miklavcic D, eds. *8th European Medical and Biological Engineering Conference*. IFMBE Proceedings. Springer International Publishing; 2021:733-739. doi:10.1007/978-3-030-64610-3_82

18. Mulavara AP, Feiveson AH, Fiedler J, Cohen H, Peters B T, Miller C, Brady R, Bloomberg J J. Locomotor function after long-duration space flight: effects and motor learning during recovery. *Exp Brain Res*. 2010;202(3):649-659. doi:10.1007/s00221-010-2171-0

19. Muscle mechanics: adaptations with exercise-training. - Abstract - Europe PMC. Accessed April 5, 2021. https://europepmc.org/article/med/8744258

20. Berzosa C, Gutierrez H, Bascuas PJ, Arbones I, Bataller-Cervero AV. Muscle Tone and Body Weight Predict Uphill Race Time in Amateur Trail Runners. *Int J Environ Res Public Health*. 2021;18(4). doi:10.3390/ijerph18042040

21. Haddad F, Herrick RE, Adams GR, Baldwin KM. Myosin heavy chain expression in rodent skeletal muscle: effects of exposure to zero gravity. *J Appl Physiol (1985)*. 1993;75(6):2471-2477. doi:10.1152/jappl.1993.75.6.2471

22. Burkhart K, Allaire B, Bouxsein ML. Negative Effects of Long-duration Spaceflight on Paraspinal Muscle Morphology. *Spine (Phila Pa 1976)*. 2019;44(12):879-886. doi:10.1097/BRS.0000000000002959

23. Agyapong-Badu S, Warner MB, Samuel D, Koutra V, Stokes M. Non-Invasive Biomarkers of Musculoskeletal Health with High Discriminant Ability for Age and Gender. *Journal of Clinical Medicine*. 2021;10(7):1352. doi:10.3390/jcm10071352

24. Loehr JA, Guilliams ME, Petersen N, Hirsch N, Kawashima S, Ohshima H. Physical Training for Long-Duration Spaceflight. *Aerospace Medicine and Human Performance*. 2015;86(12):A14-A23. doi:10.3357/AMHP.EC03.2015

25. MULAVARA, AJITKUMAR P.[1]; PETERS, BRIAN T.[1]; MILLER, CHRIS A.[1]; KOFMAN, IGOR S.[1]; RESCHKE, MILLARD F.[2]; TAYLOR, LAURA C.[1]; LAWRENCE, EMILY L.[1]; WOOD, SCOTT J.[2]; LAURIE, STEVEN S.[3]; LEE, STUART M. C.[3]; BUXTON, ROXANNE E.[4]; MAY-PHILLIPS, TIFFANY R.[3]; STENGER, MICHAEL B.[5]; PLOUTZ-SNYDER, LORI L.[6]; RYDER, JEFFREY W.[4]; FEIVESON, ALAN H.[7]; BLOOMBERG, JACOB J.[2] Physiological and Functional Alterations after Spaceflight and Bed Rest, Medicine & Science in Sports & Exercise: September 2018 - Volume 50 - Issue 9 - p 1961-1980 doi: 10.1249/MSS.0000000000001615

26. Fitts RH, Riley DR, Widrick JJ. Physiology of a Microgravity Environment Invited Review: Microgravity and skeletal muscle. *Journal of Applied Physiology*. 2000;89(2):823-839. doi:10.1152/jappl.2000.89.2.823

27. Ferrando AA, Lane HW, Stuart CA, Davis-Street J, Wolfe RR. Prolonged bed rest decreases skeletal muscle and whole body protein synthesis. *American Journal of Physiology-Endocrinology and Metabolism*. 1996;270(4):E627-E633. doi:10.1152/ajpendo.1996.270.4.E627

28. Stein TP, Leskiw MJ, Schluter MD, Donaldson MR, Larina I. Protein kinetics during and after long-duration spaceflight on MIR. *American Journal of Physiology-Endocrinology and Metabolism*. 1999;276(6):E1014-E1021. doi:10.1152/ajpendo.1999.276.6.E1014

29. Hampton S, Armstrong G, Ayyar MS, Li S. Quantification of perceived exertion during isometric force production with the Borg scale in healthy individuals and patients with chronic stroke. *Top Stroke Rehabil*. 2014;21(1):33-39. doi:10.1310/tsr2101-33

30. Garcia KM, Harrison MF, Sargsyan AE, Ebert D, Dulchavsky SA. Real-time Ultrasound Assessment of Astronaut Spinal Anatomy and Disorders on the International Space Station. *J Ultrasound Med*. 2018;37(4):987-999. doi:10.1002/jum.14438

31. LeBlanc AD, Schneider VS, Evans HJ, Pientok C, Rowe R, Spector E. Regional changes in muscle mass following 17 weeks of bed rest. *Journal of Applied Physiology*. 1992;73(5):2172-2178. doi:10.1152/jappl.1992.73.5.2172

32. A L, R R, V S, H E, T H. Regional muscle loss after short duration spaceflight. *Aviat Space Environ Med*. 1995;66(12):1151-1154.

33. Arbeille P, Chaput D, Zuj K, Depriester A, Maillet A, Belbis O, Benarroche P, Barde S. Remote Echography between a Ground Control Center and the International Space Station Using a Tele-operated Echograph with Motorized Probe. *Ultrasound Med Biol*. 2018;44(11):2406-2412. doi:10.1016/j.ultrasmedbio.2018.06.012

34. Bodine SC, Baehr LM. Skeletal muscle atrophy and the E3 ubiquitin ligases MuRF1 and MAFbx/atrogin-1. *Am J Physiol Endocrinol Metab*. 2014;307(6):E469-484. doi:10.1152/ajpendo.00204.2014

35. Ebert SM, Al-Zougbi A, Bodine SC, Adams CM. Skeletal Muscle Atrophy: Discovery of Mechanisms and Potential Therapies. *Physiology*. 2019;34(4):232-239. doi:10.1152/physiol.00003.2019

36. Steffen JM, Musacchia XJ. Spaceflight effects on adult rat muscle protein, nucleic acids, and amino acids. *American Journal of Physiology-Regulatory, Integrative and Comparative Physiology*. 1986;251(6):R1059-R1063. doi:10.1152/ajpregu.1986.251.6.R1059

37. Green DA, Scott JPR. Spinal Health during Unloading and Reloading Associated with Spaceflight. *Front Physiol*. 2018;8. doi:10.3389/fphys.2017.01126

38. Ibrahim MM. Subcutaneous and visceral adipose tissue: structural and functional differences. *Obesity Reviews*. 2010;11(1):11-18. doi:https://doi.org/10.1111/j.1467-789X.2009.00623.x

39. Technology. Myoton. Accessed April 7, 2021. https://www.myoton.com/technology/

40. Arbeille P, Zuj K, Saccomandi A, Ruiz J, Andre E, De La Porte C, Carles G, Blouin J, Georgescu M. Teleoperated Echograph and Probe Transducer for Remote Ultrasound Investigation on Isolated Patients (Study of 100 Cases). *Telemed J E Health*. 2016;22(7):599-607. doi:10.1089/tmj.2015.0186

41. Suchomel TJ, Nimphius S, Bellon CR, Stone MH. The Importance of Muscular Strength: Training Considerations. *Sports Med*. 2018;48(4):765-785. doi:10.1007/s40279-018-0862-z

42. Willard FH, Vleeming A, Schuenke MD, Danneels L, Schleip R. The thoracolumbar fascia: anatomy, function and clinical considerations. *J Anat*. 2012;221(6):507-536. doi:10.1111/j.1469-7580.2012.01511.x

43. Shriki J. Ultrasound physics. *Crit Care Clin*. 2014;30(1):1-24, v. doi:10.1016/j.ccc.2013.08.004

44. Garcia-Bernal M-I, Heredia-Rizo AM, Gonzalez-Garcia P, Cortés-Vega M-D, Casuso-Holgado MJ. Validity and reliability of myotonometry for assessing muscle viscoelastic properties in patients with stroke: a systematic review and meta-analysis. *Scientific Reports*. 2021;11(1):5062. doi:10.1038/s41598-021-84656-1